Available at
www.ComputerScienceWeb.com
POWERED BY SCIENCE @ DIRECT®

Pattern Recognition Letters 24 (2003) 607–615

Pattern Recognition Letters

www.elsevier.com/locate/patrec

# Spatio-temporal characterization of vessel segments applied to retinal angiographic images

Y. Bouaoune *, M.K. Assogba, J.C. Nunes, P. Bunel

*Laboratoire d'Etude et de Recherche en Instrumentation, Signaux et Systèmes L.E.R.I.S.S. Université Paris XII-Val de Marne, 61 Avenue du Général de Gaulle, 94010 Créteil Cedex, France*

Received 8 September 1999; received in revised form 16 August 2002

**Abstract**

In this paper, we present a new approach of analysis and recognition of retinal vessel segments for the quantification of their shapes change due to alterations. This approach is based on a spatial followed by a temporal characterization of retinal fluorescein angiographic images. The spatial characteristics (coordinates and classification number i.e. numbering of segments) are associated to bifurcation points (bp), which are matched in temporal image pairs for vessel segments correspondence forming. The matching process uses spatial and temporal characteristics between the bp and their surrounded vessel segments by computing a coefficient of similarity measurement.

The recognition of vessel segments will help ophthalmologists in quantifying changes in vessel shape parameters and detect the temporal evolution of some retinal pathologies as the Sickle Cell retinopathy in our case.


*Keywords:* Spatio-temporal characterization; Vessel segment correspondence; Retinal angiography; Sickle cell retinopathy

## 1. Introduction

The accurate and automated analysis of vessel morphology is a valuable tool in medical imaging since it is applicable to many diagnostic processes i.e. retinal fluorescein angiography (Zhou et al., 1994; Gao et al., 2000) and cine-angiography (Tolias and Panas, 1998). Such an analysis requires a spatial characterization of each image to be compared and a temporal characterization using a sequence of images for diagnostic decision making.

Blood vessel appearance is an important indicator for many diagnoses, including diabetes, hypertension and arteriosclerosis and information about retinal blood vessel morphology is used to quantify the severity and progression of a number diseases.

For example, during Sickle Cell retinopathy, a remodeling of the peripheral retinal vascular bed is observed: the retinal vessel tortuosity (relative curvature) can change due to alteration (Binaghi and Lévy, 1993) or a part of the vascular tree can

* Corresponding author. Tel.: +33-1-4517-1474; fax: +33-1-4517-1492.

*E-mail address:* bouaoune@univ-paris12.fr (Y. Bouaoune).


PII: S0167-8655(02)00280-5

disappear. One of the drawbacks of these modifications is a severe visual loss.

Up to now, to the best of our knowledge, the technique used by ophthalmologists to study vessels shape modification due to Sickle Cell retinopathy is visual and by this way qualitative. We propose an approach of analysis and recognition of their changes due to alteration (Assogba, 1999). In this paper, we focus on the problem of forming correspondences between vessel segments in temporal image pairs.

In our research, the images are supposed to be registered. A detailed survey of image registration techniques can be found in (Brown, 1992; Zana and Klein, 1999). Our registration technique (Bunel et al., 1996) is based on the detection of invariant existing structures in the images to be overlaid. The overlaying of these invariant structures allows the whole image registration. It is well known that the retinal vascular net and particularly the bifurcation points (bp) are specific anatomical landmarks. The vascular net will be taken as the control structure for the registration. An accurate superposition of two angiograms is obtained by the overlay of both vascular nets.

Our method (Koné et al., 1994) is based on automatic detection of vascular net by photometric and morphologic criteria. Vessel pixel luminance is always different from the local mean luminance and in general, vessels have a filiform aspect. The developed method proceeds from these two assumptions and depends upon given pixels simultaneously fulfilling a luminance and neighboring (connexity) criteria.

The first step of the process uses a sliding window of growing size to detect local contrasted pixels. These pixels are candidates to belong on the vessel. The window size had been chosen to be at least 3 times the artery diameter.

The second step selects candidate pixels with a morphologic criteria (belonging to linear shape objects). At the end of the process, we obtained a binary image.

The detection of features as the vascular pattern detected on each image allows to base the registration on these patterns by superposition. The registration is done in two steps: the detection of bp (landmarks) on each pattern and the matching of bp between the two patterns. The matching is done using a polygonal approach. A polynomial transformation is used to obtain the greatest number of bp in correspondence between two images.

Hence, the original technique, presented in this article, uses vessel centerlines obtained by skeletonizing the segmented vascular tree. We proceed in two main steps. The first one is a spatial characterization consisting in detecting bp in each image to be compared and labeling vessel segments around bp to which are associated image characteristics. The second step is the temporal characterization, which consists in recognizing in a pair of images, the correspondence between the bp and their surrounding vessel segments by computing a coefficient of similarity measurement.

## 2. Spatio-temporal characterization of vascular segments

The spatio-temporal characterization consists of a spatial representation of each image to be compared and then comparing the images using the bp as landmarks.

### 2.1. Spatial characterization

Firstly, the segmented vascular tree of the retinal angiographic image is skeletonizing. The skeleton is obtained by a morphological operation (erosion) where the stop criterion is the conservation of a single pixel. The structure obtained consists only of bp and vessel segments. Typically, a vessel segment is a set of connected pixels, each of which has exactly two neighbouring elements. Hence, in a top–down scanning, a point of the structure is a bp when it is surrounded by more than two pixels. The characteristics associated to bp and the linked vessels are:

Number of bp—coordinates
- Number of vessel segment
- Length of the vessel
- Coordinates of the end of the vessel
- Number of bp Link or −1 if at the end of the vessel

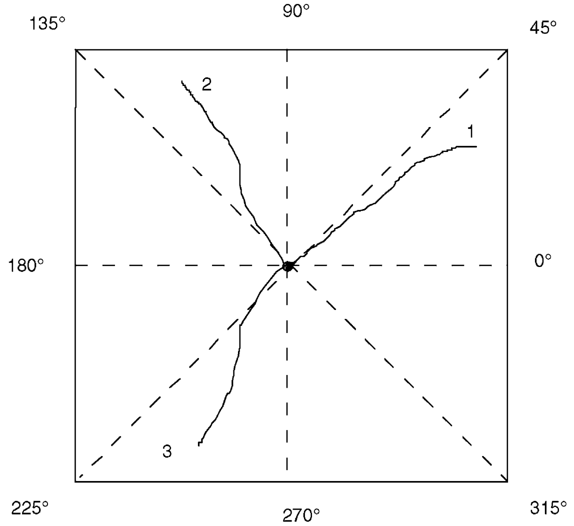


Fig. 1. Local numbering of segments.

#### 2.1.1. Number of vessels segments around a bifurcation point

As if we were using Freeman coding, the segments are ordered in counter clockwise as shown in Fig. 1.

By giving a local number, we count in the same way the number of vessel segments at each bp. This number is useful to temporal characterization as we will see.

#### 2.1.2. The classification number of vessel segments

During the scanning, the segments are given numbers according to their spatial position, counting counter clockwise. When a segment is related to two bp, it is not numbered any more at the second bp. In Fig. 2, at the bp number $M$ is related to segments $n$, $n+1$ and $n+2$. At bp $M+1$, we do not take into account segment $n+1$ when incrementing.

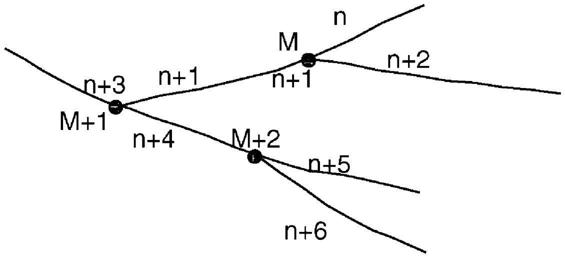


Fig. 2. Segments notation.

In short, to bp $M+2$ will be associated the following: the coordinates of bp $M+2$, vessel segment numbers $n+4$, $n+5$, $n+6$ and the number of vessel segments around bifurcation point $M+2$.

Thus, each vessel segment has a unique numbering.

### 2.2. Temporal characterization

Let $I_t$ be a reference image taken at time $t$ and $I_{t+d}$ be an image taken at $t+d$. Bear in mind that the images $I_t$ and $I_{t+d}$ have been registered with a relative accuracy.

Let $vs_1$ be a vessel segment belonging to $I_t$ and $vs_2$ a vessel segment of $I_{t+d}$. The temporal characterization of $vs_1$ consists in finding in $I_{t+d}$ its correspondent, which may be $vs_2$. For that, we look for the temporal correspondence between bp and their connected vessel segments.

#### 2.2.1. Bifurcation points matching

Let $bp_t$ be a bp of $I_t$. Let $W$ be the size of a window around $bp_t$. The size of the window is determined by a maximum constraint of displacement from one image to another. This displacement is closely related to the quality of the registration between the two images, in our case $W = 10 \times 10$ pixels.

Let *nbc* be the number of candidates inside a window of size $W$ centered on the point in $I_{t+d}$ of coordinates equivalent to the coordinates of $bp_t$.

For each candidate bp, we compute a criterion of maximum verisimilitude named similarity measurement and based on the computation of a combination on two local coefficients (directional and contrast coefficients).

Different cases are possible:

- $nbc = 0$: In this case, $bp_t$ in the image $I_t$ has no correspondence in the image $I_{t+d}$. It means that the bp has disappeared (because of the progress of the illness). The bp is matched with no correspondence.
- $nbc = 1$: The single candidate is considered as the corresponding point.

$nbc > 1$: In this case, we choose among all candidates the one getting the smallest value of similarity measurement.

*2.2.1.1. Directional coefficient*. The directional criterion is based on the computation of the differences of direction between vessel segments. Let $l_p$ be the perimeter of the window of size $W'$ (5 pixels × 5 pixels). The direction of a segment is defined as the position at which the segment crosses the periphery of the window. In our example, the perimeter of the window is $l_p = 16$.

Fig. 3 depicts the direction of segments.

If a segment around $\mathrm{bp}_t$ crosses the periphery at $x$ and a segment around $\mathrm{bp}_{t+d}$ crosses it at $x'$, the absolute value of the difference $|x - x'|$ is considered as the directional difference of the two segments. Let $\alpha_1, \alpha_2, \ldots, \alpha_N$ be the directional differences of vessel segments around $\mathrm{bp}_t$ and a candidate in $I_{t+d}$.

For the calculus, if $x > (l_p/2)$ and $x' < (l_p/2)$, $x$ takes the value $x - l_p$ and reverse. For example, if $x = 15$ and $x' = 0$, the modulus of the difference is equal to 1.

In Fig. 3, vessel segments of one of the bp are in bold and the differences are $\alpha_1 = 3$; $\alpha_2 = 2$; $\alpha_3 = 2$.

The two bp will match at the condition $\sum_{k=1}^{N} \alpha_k \to 0$, $N$ is the number of couple of segments used to measure the $\alpha_k$ values.

Using previous condition, we have defined the following directional coefficient (dc) for matching two bp $(\mathrm{bp}_t, \mathrm{bp}_{t+d})$:

$$\mathrm{dc}(\mathrm{bp}_t, \mathrm{bp}_{t+d}) = \frac{1}{N} \sum_{k=1}^{N} \alpha_k$$

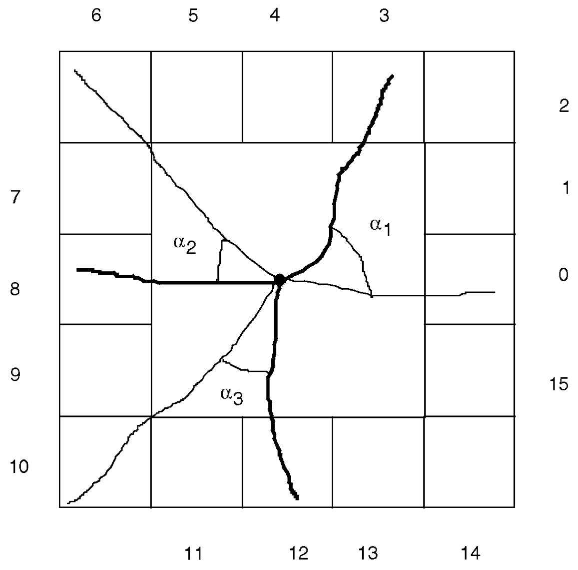


Fig. 3. Direction of segments.

$$cc(\mathrm{bp}_t, \mathrm{bp}_{t+d}) = \frac{\sum_{x'=-W/2}^{W/2} \sum_{y'=-W/2}^{W/2} I_t(x + x', y + y') I_{t+d}(x_d + x', y_d + y')}{\sqrt{\sum_{x'=-W/2}^{W/2} \sum_{y'=-W/2}^{W/2} I_t^2(x + x', y + y') \sum_{x'=-W/2}^{W/2} \sum_{y'=-W/2}^{W/2} I_{t+d}^2(x_d + x', y_d + y')}}$$

It can appear that the number of line segments of a junction evolves in time. A junction with 4 line segments can be thus transformed into a junction with 3 line segments. When this case is encountered, correspondence between line segments is analyzed by testing all the possible combinations between a set of 4 elements and a set with 3 elements.

Selected associations will be those which minimize the preceding relation among all the possible solutions.

*2.2.1.2. Contrast coefficient*. Using binary images (skeleton images), we process the inter-correlation between supposed matched bp.

The contrast coefficient between two bp can be expressed as:

where $\mathrm{bp}_t$ is a bp with $(x, y)$ coordinates in image $I_{t+d}$ and $\mathrm{bp}_{t+d}$ is a bp with $(x_d, y_d)$ coordinates in image $I_{t+d}$.

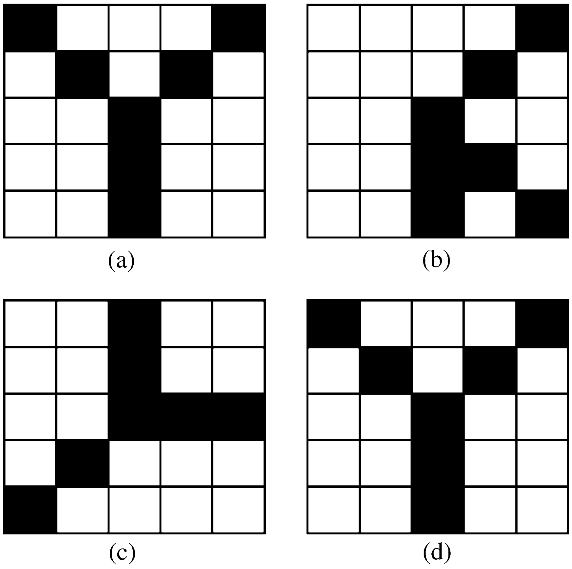


Fig. 4. Binary representation of different bp.

This coefficient characterizes an intensity measurement as its gets closer to 1 when both candidates $bp_t$ and $bp_{t+d}$ represent a growing contrast of similarity.

Fig. 4 illustrates the computation technique. Fig. 4a is to be computed with respectively Fig. 4b–d.

In our example, $I_t(x, y)$ is applied to Fig. 4a and $I_{t+d}(x_d, y_d)$ is applied to Fig. 4b–d. The results are 0.2 between Fig. 4a and b, 0.142 between Fig. 4a and c and 1 between Fig. 4a and d.

*2.2.1.3. Similarity measurement*. These two coefficients (directional and contrast) are combined to obtain a local measurement which indicate the similarity between the two bp, similarity in direction and contrast.

This measure is expressed as:

$$sm(\mathrm{bp}_t, \mathrm{bp}_{t+d}) = (1 - cc(\mathrm{bp}_t, \mathrm{bp}_{t+d})) + \mathrm{dc}(\mathrm{bp}_t, \mathrm{bp}_{t+d})$$

The lower value of this measurement is, the greater similarity between the two bp is.

When there is two or more candidates, this value allows us to discriminate between them.

In our work, the algorithm creates a result file: For each bifurcation point of the image $I_t$, we note its correspondent in the image $I_{t+d}$ and around each bp, we have associated the surrounded segments.

If a vessel segment has completely disappeared due to an occlusion for example, the algorithm detects an absence of the correspondent segment.

In the same way, if a bp and their vessel segments disappeared in the image $I_{t+d}$ due to the progress of the pathology, the algorithm detects it and marks no correspondence for this particular case.

## 3. Results and discussion

Our goal is to develop a method to help ophthalmologists to make quantitative diagnostic of modifications in vessel segments shape parameters.

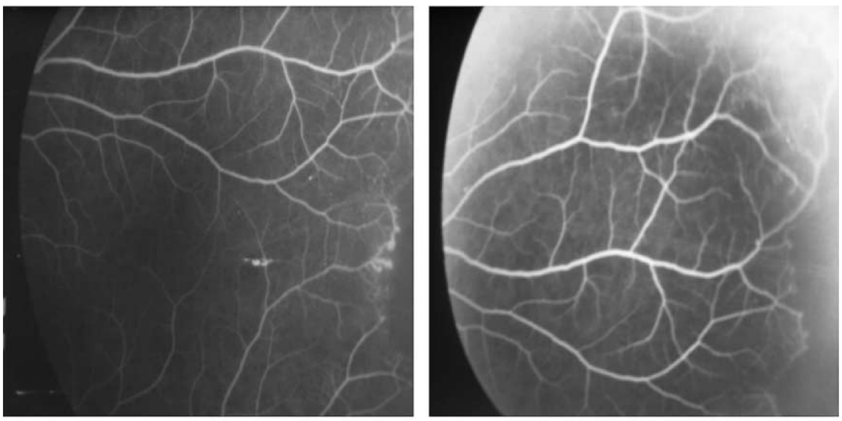

(a) (b)

Fig. 5. Images of a patient: (a) $I_t$ and (b) $I_{t+d}$.

We used fluorescein angiographic images, digitized from photographic images at a resolution of $512 \times 512$ pixels and with a quantization of 8 bits per pixel.

We have tested the performance of the developed system and we show our results on a couple of angiographic images (Fig. 5).

Fig. 5 presents two temporal retinal fluorescein angiographic images.

After registration (Fig. 6) and then segmentation of the vascular trees, the skeletonizing is done as shown on Fig. 7 on the filtered images.

For each skeleton's image and for each bp, we obtain a result file with this structure: Here is an extract of our results:

| Number of bp | | Coordinates of the bp | | Number of bp | | Coordinates of the bp | |
|---|---|---|---|---|---|---|---|
| Number of vessel segment | Length | Coordinates of the end of the vessel | Number of bp's link or −1 if end of vessel | Number of vessel segment | Length | Coordinates of the end of the vessel | Number of bp's link or −1 if end of vessel |
| 21 | | (194, 186) | | 29 | | (270, 204) | |
| *Image $I_t$* | | | | *Image $I_{t+d}$* | | | |
| 52 | 9 | (203, 182) | −1 | 60 | 67 | (337, 219) | 32 |
| 47 | 60 | (138, 153) | 18 | 39 | 32 | (172, 138) | 18 |
| 53 | 29 | (207, 215) | 23 | 61 | 52 | (267, 256) | 44 |
| 22 | | (268, 203) | | 30 | | (391, 209) | |
| *Image $I_t$* | | | | *Image $I_{t+d}$* | | | |
| 54 | 69 | (337, 219) | 24 | 57 | 19 | (393, 202) | 28 |
| 55 | 163 | (107, 113) | −1 | 62 | 10 | (382, 214) | −1 |
| 56 | 56 | (254, 257) | −1 | 63 | 6 | (393, 215) | −1 |
| 23 | | (209, 217) | | 31 | | (414, 214) | |
| *Image $I_t$* | | | | *Image $I_{t+d}$* | | | |
| 57 | 15 | (224, 224) | 25 | 64 | 11 | (425, 216) | −1 |
| 53 | 29 | (194, 186) | 21 | 57 | 19 | (393, 202) | 28 |
| 58 | 35 | (204, 251) | −1 | 65 | 6 | (414, 220) | −1 |
| 24 | | (339, 219) | | 32 | | (339, 219) | |
| *Image $I_t$* | | | | *Image $I_{t+d}$* | | | |
| 48 | 67 | (405, 175) | 19 | 66 | 43 | (382, 190) | −1 |
| 54 | 69 | (268, 203) | 22 | 60 | 67 | (270, 204) | 29 |
| 59 | 66 | (402, 252) | 27 | 67 | 62 | (397, 258) | 45 |
| 25 | | (226, 224) | | 33 | | (215, 224) | |
| *Image $I_t$* | | | | *Image $I_{t+d}$* | | | |
| 60 | 24 | (249, 214) | −1 | 68 | 15 | (230, 229) | 34 |
| 57 | 15 | (209, 217) | 23 | 51 | 91 | (142, 164) | 24 |
| 61 | 5 | (231, 226) | −1 | 69 | 24 | (211, 248) | 42 |
| 26 | | (414, 246) | | 34 | | (232, 229) | |

| *Image $I_t$* | | | | *Image $I_{t+d}$* | | | |
|---|---|---|---|---|---|---|---|
| 62 | 20 | (433, 236) | −1 | 70 | 2 | (234, 227) | −1 |
| 63 | 8 | (406, 250) | 27 | 68 | 15 | (215, 224) | 33 |
| 64 | 1 | (415, 247) | −1 | 71 | 8 | (239, 236) | −1 |

and so on.

These results are combined with the file indicating the similarity coefficient between two bp. If two or more bifurcation points are candidates, we choose which one has the smallest value of similarity measurement.

| Image $I_t$ | | Image $I_{t+d}$ | | Similarity's coefficient |
|---|---|---|---|---|
| Number of bp | $(x, y)$ | Number of bp | $(x, y)$ | |
| 21 | (194, 186) | No correspondent | | |
| 22 | (268, 203) | 29 | (270, 204) | 1.42 |
| 23 | (209, 217) | 33 | (215, 224) | 0.00 |
| 24 | (339, 219) | 32 | (339, 219) | 0.50 |
| 25 | (226, 224) | 34 | (232, 229) | 0.00 |
| 26 | (414, 246) | No correspondent | | |

and so on.

On the first image, the bp numbered 21 has not correspondence. On another side, the bp numbered 25 has a correspondent numbered 34 in the second image with a very good similarity coefficient. We conclude that the two bp 25 and 34 are in correspondence. By this way, we can associate the segments surrounded the bp and confirm our preliminary results (the two bp 23 and 33 are in correspondence and the segments 57 and 68 are associated).

| Image $I_t$ | | | | Image $I_{t+d}$ | | | |
|---|---|---|---|---|---|---|---|
| 25 | | (226, 224) | | 34 | | (232, 229) | |
| 60 | 24 | (249, 214) | −1 | 70 | 2 | (234, 227) | −1 |
| 57 | 15 | (209, 217) | 23 | 68 | 15 | (215, 224) | 33 |
| 61 | 5 | (231, 226) | −1 | 71 | 8 | (239, 236) | −1 |

By this way, we built a hierarchical tree, for each image and their correspondences, where a difference or a lacuna in the sequence indicates a change between the two compared images.

To improve this method, we will add more criteria as diameter (the diameter of the vessel segment is determined thanks to the number of erosions carried out), eccentricity ...) for a best characterization of each vessel segment and his variation. The length alone is not sufficient to measure completely the modification. Also, we will use the graph theory (Hivernat et al., 1998; Diestel, 2000) to describe, organize the vascular tree into a hierarchy and thus improve the comparison.

Furthermore, the visualization of the differences between the images will be more easier.

## 4. Conclusion

There exists an important number of situations or diseases, which are followed by changes in vessels shape parameters such as length, diameter and tortuosity. These diseases can damage vision. Up to now, diagnosis made by ophthalmologists of the changes due to retinal vessel alterations have

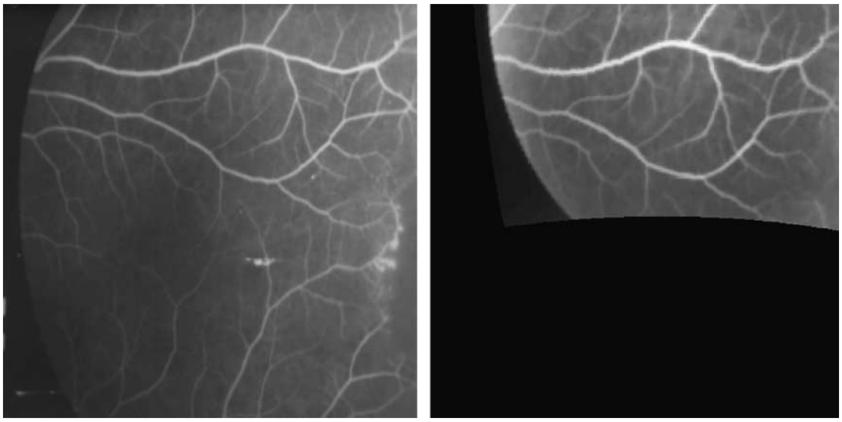

Fig. 6. Registered images.

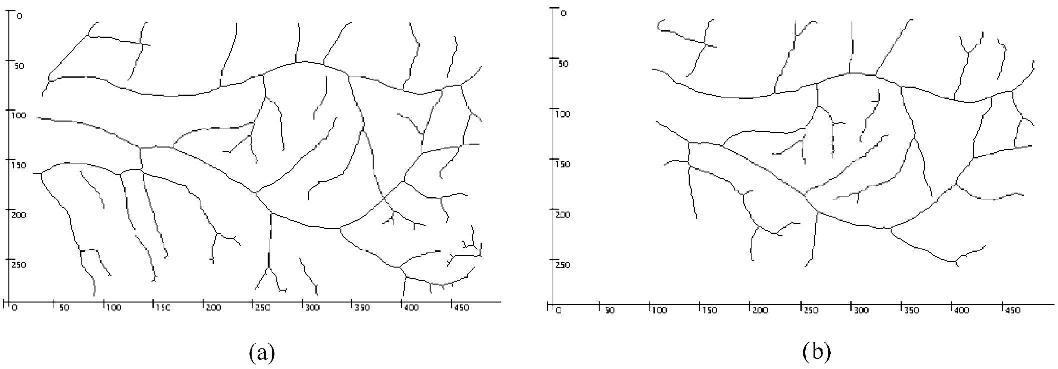


Fig. 7. Skeletons of the vascular trees: (a) image $I_t$ and (b) image $I_{t+d}$.

been visual and therefore subjective. Now, we have introduced a precise objective method for solving correspondence problems of vessel segments. The spatial characterization of vascular structure performs well. The temporal characterization consists in matching bp and afterwards the forming vessel segments correspondence.

We have developed a correspondence simple method; however, the quality of the image acquisition, the segmentation of the vascular trees and the registration can limit the correspondence formed between the segment vessels.

We continue our research with the study of the diameter and the tortuosity of each vessel in the goal to improve the method and quantify accurately the changes in retinal shape parameters in order to detect changes and temporal evolution of some pathologies as the Sickle Cell retinopathy.

## Acknowledgements

We would like presenting our acknowledgements to Doctor M. BINAGHI from the "Clinique Ophtalmologique" of the "Centre Hospitalier Universitaire Henri Mondor", Créteil, France.

## References

Assogba, K., 1999. Analyse et reconnaissance des formes des vaisseaux rétiniens pour la quantification de leurs modifications. Thèse de Doctorat de 3ème Cycle—Université Paris XII.

Binaghi, M., Lévy, C., 1993. Œil et hémoglobinopathies. Editions Techniques. Encycl. Med. Chir. (Paris–France). Ophtalmologie, 21-452-G-20.

Brown, L.G., 1992. A survey of image registration techniques. ACM Comput. Surveys 24 (4), 325–376.

Bunel, P., Koné, T., Mimoun, G., Bouaoune, Y., Coscas, G., 1996. Fully Automatic Digital Overlaying on Retinal Fluorescein Angiograms. 10th Nordic-Baltic Conference on Biomedical Engineering. Tampere, Finland.

Diestel, V., 2000. Graph theory. Graduate Texts in Mathematics, Vol. 13, Springer-Verlag, Berlin.

Gao, X.W., Bharath, A., Stanton, A., Hughes, A., Chapman, N., Thom, S., 2000. Quantification and characterisation of arteries in retinal images. Comput. Meth. Prog. Biomed. 63 (2), 133–146.

Hivernat, C., Descombes, X., Randriamasy, S., Zerubia, J., 1998. Mise en correspondance et recalage de graphes: Application aux réseaux routiers extraits d'un couple carte/image. Rapport de Recherche, no. 3529, Inria, Sophia, Antipolis.

Koné, T., Mimoun, G., Bunel, P., Meunier, I., Coscas, G., 1994. New Method for Automatic Retinal Vessels Detection on Digitized Fluorescein Angiography. Conference of Association for Research in Vision and Ophthalmology (ARVO). Sarasota, FL, USA.

Tolias, Y., Panas, S., 1998. A fuzzy vessel tracking algorithm for retinal images based on fuzzy clustering. IEEE Trans. Med. Imaging 17 (2), 263–273.

Zana, F., Klein, J.C., 1999. A multimodal registration algorithm of eye fundus images using vessels detection and hough transform. IEEE Trans. Med. Imaging 18 (5), 419–428.

Zhou, L., Rzeszotarski, M.S., Singerman, L.J., Chokreff, J.M., 1994. Detection and quantification of retinopathy using digital angiograms. IEEE Trans. Med. Imaging 13 (4), 619–626.